

Calculation of ohmic resistance effects in rectangular electrodes of finite thickness

S. L. MARSHALL, S. K. WOLFF

Department of Chemistry, University of Western Australia, Nedlands, WA 6009, Australia

Received 19 November 1991; revised 27 May 1992

The current distribution in electrochemical cells consisting of parallel rectangular plates is determined. The calculations involve the evaluation of the appropriate analytical solution of Laplace's equation within the electrodes and electrolyte, with boundary conditions corresponding to potential continuity (primary current distribution) or linear electrode kinetics (secondary current distribution) at the electrode–electrolyte interface, and do not make the usual assumption that current flow in the resistive electrode is one-dimensional. The current distributions are given in the form of Fourier series that allow the effects of electrode resistance and electrical contact geometry to be determined.

1. Introduction

In theoretical treatments of electrochemical cells, it is generally assumed (with complete justification in many cases) that electrode resistance is negligible. As a result, consideration of cells made up of resistive electrodes has received relatively little attention in the literature. The presence of electrodes with finite resistivity significantly complicates not only the analysis of current and potential distribution, but also factors such as electrode-kinetic and hydrodynamic/mass transport effects.

Existing treatments of electrode resistivity are mostly based on the assumption of a one-dimensional current distribution within the resistive electrode. The work of Tobias and Wijnsman [1] was based on the calculation of the stream function by summation of Fourier series. More recent treatments have involved combination of Ohm's law with an appropriate electrode kinetic equation to set up a current balance condition, relating the current flowing into and out of each element of the resistive electrode to the local overpotential. This conservation law takes the form of a second-order differential equation, for which analytical solutions may be obtained in favourable cases. Thus, Conway *et al.* [2] and Rangarajan *et al.* [3] determined the potential distribution in wires under linear and exponential kinetic approximations. Scott [4] and Robertson [5] expressed the potentials in resistive parallel-plate electrodes as solutions of a Helmholtz-type differential equation. Nonlinear (Butler–Volmer) kinetics coupled with mass-transport effects were analysed numerically in a study of wire plating by Alkire and Varjian [6, 7], and in a recent paper by Lanzi and Landau [8] the implications of the Tafel approximation were considered. Finite difference and related techniques have been applied by Vaaler [9] and by Rousar *et al.* [10] to the calculation of two and three-dimensional resistive-electrode potential distributions in mesh electrodes for chlor-alkali cells, with the assumption that the potential is determined by Ohm's

law rather than Laplace's equation. Recent work by Bisang and Kreysa [11] and Bisang [12] involved calculation of the current distribution in a cylindrical cell consisting of a resistive rod (in which the current distribution is one-dimensional) surrounded by a tube of uniform potential.

The advantage of the current-balance approach used in the above analyses of one-dimensional systems [2–8, 11, 12] is that it is relatively straightforward to incorporate nonlinear electrode kinetics [2, 3, 8] and mass-transport effects [6, 7]. The main disadvantage is that the restriction of this approach to resistive electrodes with one-dimensional current flow makes it more difficult to solve the important practical problems of determining the range of cell geometries for which such resistive effects are expected to be important, and estimating the perturbative effect of contact geometry on the current distribution.

The most general current-balance condition that can be applied to a three-dimensional source-free conductor is expressed by Laplace's equation. Thus, the use of Ohm's law [9, 10] and the assumption of a one-dimensional current distribution [1–7] are best regarded as approximations to more general problems in which the potentials in the electrode and electrolyte are both determined by the solution of Laplace's equation.

The subject of the present paper is the application of Laplace's equation to the calculation of electrode resistance effects on the primary and secondary current distribution between two parallel plates, the latter distribution being determined subject to the additional assumption of linear electrode kinetics at the resistive electrode. Our main aim is to illustrate the general method of calculation rather than to develop an accurate model of a specific electrochemical system, but we note that the electrode configuration assumed here is of some relevance to the design of tank electrolyzers. It will be shown how the primary and secondary current distributions depend on the electrolyte: electrode conductivity ratio, and on geometrical

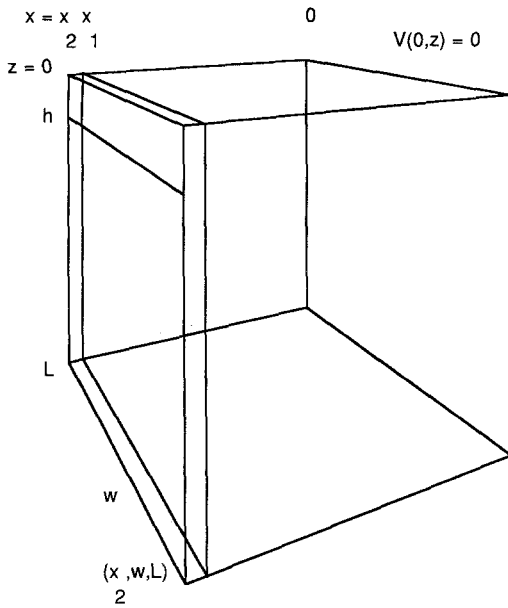


Fig. 1. Diagram of the rectangular cell, showing definition of geometrical parameters. The electrode in the plane $x = 0$ is assumed to be equipotential.

characteristics of the cell such as the thickness : length ratio for the electrode.

2. Primary current distribution

2.1. Mathematical statement of the problem

The cell, shown in Fig. 1, consists of two parallel plates of length L and width w , one of which is bounded by the planes $x = x_1$ and $x = x_2$. The other plate electrode, which lies in the plane $x = 0$, is assumed to be sufficiently thick that its potential is uniform. Electrical contact to the outer surface of the resistive electrode is made through a narrow band of width h , across which the total current I through the cell is assumed to be uniformly distributed. The remainder of the surface $x = x_2$ and the two end surfaces $z = 0$ and $z = L$, $0 < x < x_2$, are insulated. The primary current distribution is derived from a potential $V(x, z)$ that satisfies the two-dimensional rectangular form of Laplace's equation

$$\nabla^2 V \equiv \frac{\partial^2 V}{\partial x^2} + \frac{\partial^2 V}{\partial z^2} = 0 \tag{1}$$

in the regions $0 < x < x_1$ (conductivity κ_2) and $x_1 < x < x_2$ (conductivity κ_1). This equation states that the total amounts of current flowing into and out of a given element of conductor are equal. Boundary conditions to be satisfied by V are as follows:

$$V(0, z) = 0 \tag{2}$$

$$\lim_{x \downarrow x_1} V(x, z) = \lim_{x \uparrow x_1} V(x, z) \tag{3}$$

$$\lim_{x \downarrow x_1} \kappa_2 \frac{\partial V}{\partial x}(x, z) = \lim_{x \uparrow x_1} \kappa_1 \frac{\partial V}{\partial x}(x, z) \tag{4}$$

$$\frac{\partial V}{\partial x}(x_2, z) = \frac{-I/\kappa_1}{hw} f(z) \tag{5}$$

where $f(z) = 1, 0 < z < h$, and $f(z) = 0, h < z < L$.

$$\frac{\partial V}{\partial z}(x, 0) = \frac{\partial V}{\partial z}(x, L) = 0 \tag{6}$$

Equations 3 and 4 state that the potential and current density are continuous across the surface $x = x_1$. Equation 3 is true if the surface overpotential is zero, as assumed here.

2.2. Analytical solution

The solution to this boundary value problem can be found by application of standard methods (Fourier series and separation of variables) as described, for example, by Moon and Spencer [13]. Thus, the solution is assumed to consist of terms of the form

$$V(x, z) = X(x)Z(z) \tag{7}$$

On substitution of this expression into Equation 1, the differential equations satisfied by the X and Z functions are found to be:

$$X'' - \lambda^2 X = 0 \tag{8}$$

$$Z'' + \lambda^2 Z = 0 \tag{9}$$

where λ is a constant. The form of the solutions to these equations depends on whether $\lambda^2 = 0$ or $\lambda^2 > 0$. For $\lambda = 0$, possible solutions are

$$X = 1, x \tag{10}$$

$$Z = 1, z \tag{11}$$

Insulation of the end surfaces in this case requires that $Z = 1$, so that the potential in this case depends only on x . For $\lambda^2 > 0$, Equation 6 requires that $\lambda = a_m = m\pi/L, m = 1, 2, \dots$. Possible solutions in this case are

$$X = \cosh(a_m x) \sinh(a_m x) \tag{12}$$

$$Z = \cos(a_m z) \tag{13}$$

The general solution for V is therefore expected to be of the form:

$$V(x, z) = E_0 X_0(x) + \sum_{m=1}^{\infty} E_m X_m(x) \cos(a_m z) \tag{14}$$

where X_0 is a linear function, X_m is a linear combination of hyperbolic functions, and the constants $E_m, m = 0, 1, 2, \dots$ are to be determined from the boundary conditions as described below.

The form of both X_0 and X_m is different on each side of the interface $x = x_1$. A suitable form for X_0 is

$$\begin{aligned} X_0(x) &= A_0 + B_0 x & x_1 < x < x_2 \\ &= C_0 x & 0 < x < x_1 \end{aligned} \tag{15}$$

and for $m > 0, X_m$ may be taken to be:

$$\begin{aligned} X_m(x) &= A_m \cosh(a_m x) + B_m \sinh(a_m x) & x_1 < x < x_2 \\ &= C_m \sinh(a_m x) & 0 < x < x_1 \end{aligned} \tag{16}$$

where the constants A_m, B_m and C_m must be determined

by applying the boundary conditions. To simplify the subsequent manipulations involving the Fourier series associated with the specification of the current density on the outer surface, these constants can be chosen so that $X'_m(x_2) = 1$. For $m = 0$, this requires that

$$B_0 = 1 \quad (17a)$$

There is no loss of generality here, since any constant multiple of the functions in Equation 16 will also satisfy Equation 8. (See [13], p. 188 *ff.*, for application of this procedure to other potential distribution problems). Continuity of the potential and current density across the interface, as expressed by Equations 3 and 4, respectively, yields two further equations for A_0 and C_0 :

$$C_0 = \frac{\kappa_1}{\kappa_2} B_0 \quad (17b)$$

$$A_0 + B_0 x_1 = C_0 x_1 \quad (17c)$$

from which it follows that

$$A_0 = \left(\frac{\kappa_1}{\kappa_2} - 1 \right) x_1 \quad (18a)$$

$$C_0 = \frac{\kappa_1}{\kappa_2} \quad (18b)$$

Similarly, application of the condition that $X'_m(x_2) = 1$ to the first form of Equation 16 (for $m > 0$) yields the equation

$$A_m \sinh(a_m x_2) + B_m \cosh(a_m x_2) = 1/a_m \quad (19a)$$

and the continuity conditions, Equations 3 and 4, result in

$$A_m \cosh(a_m x_1) + B_m \sinh(a_m x_1) = C_m \sinh(a_m x_1) \quad (19b)$$

$$A_m \sinh(a_m x_1) + B_m \cosh(a_m x_1) = \frac{\kappa_2}{\kappa_1} C_m \cosh(a_m x_1) \quad (19c)$$

The solution of Equations 19 (a-c) is

$$A_m = \left(1 - \frac{\kappa_2}{\kappa_1} \right) \cosh(a_m x_1) / a_m D_m \quad (20a)$$

$$B_m = \left[\sinh^2(a_m x_1) - \frac{\kappa_2}{\kappa_1} \cosh^2(a_m x_1) \right] / a_m D_m \quad (20b)$$

$$C_m = [\cosh^2(a_m x_1) - \sinh^2(a_m x_1)] / a_m D_m \equiv \frac{1}{a_m D_m} \quad (20c)$$

where D_m is the determinant

$$D_m = \left(1 - \frac{\kappa_2}{\kappa_1} \right) \sinh(a_m x_2) \sinh(a_m x_1) \cosh(a_m x_1) - \cosh(a_m x_2) \left[\sinh^2(a_m x_1) - \frac{\kappa_2}{\kappa_1} \cosh^2(a_m x_1) \right]$$

It remains to determine the coefficients E_m in Equation 14 by considering the variation of the

current density over the outer surface of the plate. From the theory of Fourier series [14], it follows that

$$E_0 = - \frac{I/\kappa_1 \int_0^L f(z) dz}{hw \int_0^L dz} = - \frac{I}{\kappa_1 Lw} \quad (21a)$$

and, for $m > 0$,

$$E_m = - \frac{I \int_0^L f(z) \cos(a_m z) dz}{\kappa_1 hw \int_0^L \cos^2(a_m z) dz} = \frac{-2I \sin(a_m h)}{\kappa_1 h L w a_m} \quad (21b)$$

The potential distribution may be conveniently expressed in dimensionless form as

$$\Phi(x, z) = \Phi_0(x) - 2 \left(\frac{\kappa_2}{\kappa_1} \right) \sum_{m=1}^{\infty} P_m(x) \times \frac{\sin(a_m h) \cos(a_m z)}{a_m h a_m w} \quad (22)$$

where

$$\Phi(x, z) = \frac{L\kappa_2}{I} V(x, z)$$

$$\Phi_0(x) = \frac{L\kappa_2}{I} E_0 X_0(x) = - \frac{x}{w} \quad 0 < x < x_1$$

$$= - \frac{x_1}{w} - \frac{\kappa_2}{\kappa_1} \left(\frac{x - x_1}{w} \right) \quad x_1 < x < x_2$$

$$P_m = a_m X_m(x)$$

Physically, the linear component Φ_0 is the potential distribution that would result from uniform distribution of current over the outer surface of the resistive plate (that is, if h were equal to L). The Fourier series expresses the deviation from this one-dimensional distribution that arises from the shape of the electrical contact and is propagated into the electrolyte through the plate of finite conductivity. The qualitative effect of the plate conductivity on the potential distribution can be clearly seen from Equation 22, for as κ_1 tends to infinity, the Fourier series contribution vanishes and the purely linear current distribution Φ_0 remains.

2.3. Calculations

The Fourier series in Equation 22 can be shown to converge by application of well-known theorems of higher analysis [13, 14], but it does not converge rapidly enough to be evaluated directly. Slowness of convergence tends to be a general property of Fourier series and is particularly pronounced for those series arising in the solution of partial differential equations with discontinuous boundary conditions (such as those expressed by Equation 5). Various convergence-acceleration schemes have been devised. The method used in the present work, which is due to Lanczos ([15], p. 61 *ff.*; see also [16]), is based on smoothing by taking a moving average of the increasingly oscillatory functions $\cos(a_m z)$. When applied to potential-distribution problems, the computational effort and

accuracy of this method compare very favourably with corresponding finite-difference calculations. Its numerical implementation is not so straightforward, however, and will be the subject of a forthcoming paper.

The potential was calculated at a 40×50 grid of points (x, z), and the equipotential curves presented below were calculated by linear inverse interpolation. All calculations were carried out on an Apple Macintosh II ci computer.

We shall illustrate the application of the above analytical result to a cell for which $x_1/L = 0.05$, $x_2/L = 0.051$, $h/L = 0.01$ and $w/L = 0.1$. A cell of this configuration could arise, for example, in the plating of a thin metallic strip. The equipotentials of the potential distribution within the electrolyte, calculated from the above expression for $\Phi(x, z)$ and an electrolyte-to-electrode conductivity ratio of 0.0001 are shown in Fig. 2. The surface $x = x_1$ is seen to deviate appreciably from being an equipotential. In the limiting case where the electrode is of infinite conductivity, the equipotentials would be vertical lines corresponding to a single value of x .

The conductivity ratio used in Fig. 2 is approximately what would be expected for molten-salt electrolytes used in some specialized plating processes at high temperatures. For aqueous electrolytes the ratio is typically much smaller. In Fig. 3, the calculations of Fig. 2 are repeated with a conductivity ratio of 0.00001; even with this lower value, the distortion of the equipotential lines is still noticeable. The favourable effect of a highly conducting electrode material can, of course, be cancelled out by the thinness of the electrode. Thus, the potential distribution in a cell of this type with $x_2/L = 0.0501$ and conductivity ratio 0.00001 is the same as that shown in Fig. 2. Evidently, the nonuniform (Fourier series) component of the general solution (Equation 22) becomes important not only when the conductivity ratio is large, but also when x_1 approaches x_2 , for in this latter case the determinant D_m of the linear equations defining A_m , B_m , and C_m approaches zero. It is worth remarking that, in practice, electrode resistance effects are more likely to result from thinness of the electrodes than conductivity ratio. The value 0.00001 used in Fig. 3 represents an upper limit to what would be expected in many cases; for example, for lead ($\kappa_1 \approx 5 \times 10^4 \Omega^{-1} \text{cm}^{-1}$ and 20% KOH ($\kappa_2 \approx 0.5 \Omega^{-1} \text{cm}^{-1}$) at about 15°C. For this particular conductivity ratio, we can see from Fig. 3 that for a thickness:length ratio of 0.001 or greater, electrode resistance effects can be neglected and one-dimensional current flow assumed.

In [4], where one-dimensional current flow in the resistive electrode was assumed, the significant parameter is a dimensionless group containing the electrode and electrolyte conductivities and certain geometrical parameters. In the present analysis, we considered it preferable to investigate separately the effects of the thickness and conductivity of the electrodes. An important feature of our work is that the

influence of external contact geometry on the shape of the current distribution within the electrolyte and the potential profile along the interface can also be determined, since this is expressed by the Fourier coefficients for the function $f(z)$. Such terminal effects cannot be investigated by the methods described in the literature [1–12].

Equation 22 also demonstrates how the width of the cell influences both the linear and nonlinear components of the potential distribution. From the expression for Φ_0 , it is clear that increasing the width of the cell will result in a smaller average potential drop between the electrodes. This is what one would expect, since the current density applied to the outer electrode would be lower. The Fourier series is seen to be reduced by the same factor, since its terms are all inversely proportional to w . The width of the cell therefore influences the *value* of the potential but has no effect on the *shape* of the potential distribution.

The above results could be used to determine the relation between the electrode thickness and the conductivity ratio for which the potential deviation along the surface $x = x_1$ is less than some prescribed value. It would be more useful, however, to include explicitly the electrode kinetic parameters in the boundary conditions defining the potential distributions in the electrode and electrolyte phases. This requires determination of the secondary current distribution, which is the subject of the next section.

3. Secondary current distribution

3.1. Electrode kinetics

The current density across an electrode is very often assumed to be related to the interfacial potential difference by the Butler–Volmer kinetic equation:

$$\frac{i}{i_0} = \exp\left(\frac{\alpha_a F \eta}{RT}\right) - \exp\left(-\frac{\alpha_c F \eta}{RT}\right) \quad (23)$$

$$\cong \frac{(\alpha_a + \alpha_c) F \eta}{RT} \quad (24)$$

in which $\alpha_{a,c}$ are the anodic and cathodic transfer coefficients, i_0 is the exchange current density, the overpotential η is the departure of the interfacial potential difference from its equilibrium value, and the other symbols have their usual significance. As recently shown by Marshall [17] the relative error resulting from the linearization of Equation 23, *viz.*

$$E = 1 - \frac{(\alpha_a + \alpha_c) F \eta / RT}{\exp\left(\frac{\alpha_a F \eta}{RT}\right) - \exp\left(-\frac{\alpha_c F \eta}{RT}\right)} \quad (25)$$

does not exceed 1% if i/i_0 is less than about 0.03. In the present work, we shall assume the validity of the linear polarization law because it allows us to determine analytically the influence of kinetic parameters on the secondary current distribution. From the practical point of view, we can regard Equation 24 as appropriate for a plating process operating at fairly low

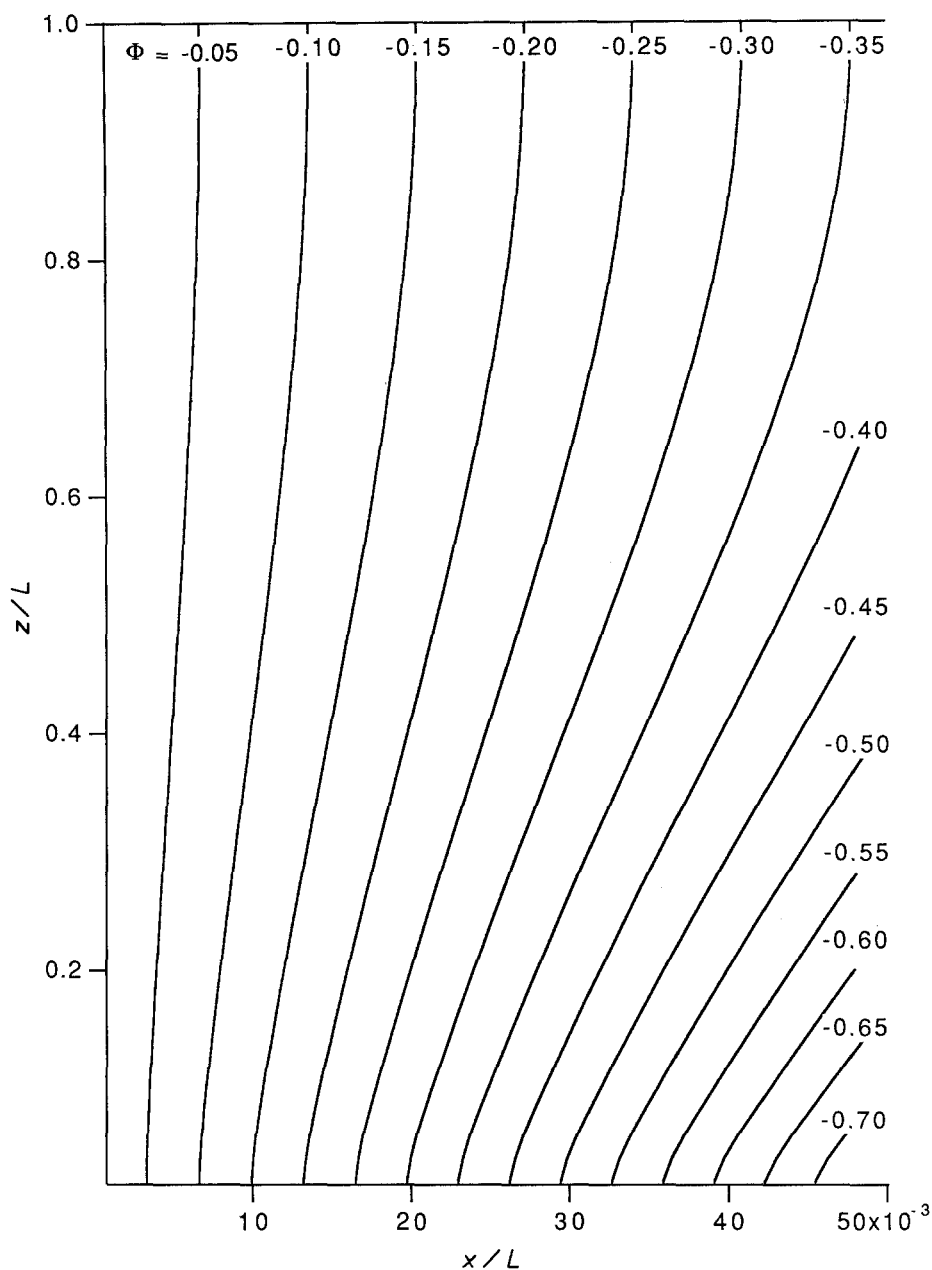


Fig. 2. Equipotentials of the potential distribution calculated from Equation 22, for $x_1/L = 0.05$, $x_2/L = 0.051$, $h/L = 0.01$, $w/L = 0.1$, and $\kappa_2/\kappa_1 = 0.0001$.

current densities (10 to 100 mA cm^{-2}) to avoid formation of dendritic deposits. This condition is quite likely to be realized in metal electrodeposition reactions in molten salts, since these are known [18] to have very high exchange current densities (usually several A cm^{-2}).

The inclusion of the equilibrium potential, V_{eq} , into the analysis is readily achieved by the addition of V_{eq} to the expression for V within the electrode, since V_{eq} also (trivially) satisfies Laplace's equation. When this is done, the potential evidently assumes its equilibrium value throughout the electrode when the total current I vanishes, since all the other terms in the potential distribution $V(x, z)$ are proportional to I . This constant potential cancels out when the overpotential is determined by subtraction of V_{eq} from the potential difference between the two phases. We can therefore equate the overpotential to the

difference in potential across the cathode-electrolyte interface.

3.2. Mathematical statement of the problem

The secondary current distribution is the solution of Laplace's equation that obeys boundary conditions expressed by Equations 2, 4, 5 and 6, and in place of Equation 3,

$$\begin{aligned} -\kappa_1 \lim_{x \downarrow x_1} \frac{\partial V}{\partial x}(x, z) &= -\kappa_2 \lim_{x \uparrow x_1} \frac{\partial V}{\partial x}(x, z) \\ &= K \left[\lim_{x \uparrow x_1} V(x, z) - \lim_{x \downarrow x_1} V(x, z) \right] \end{aligned} \quad (26)$$

where K is the slope of the polarization curve ($\Omega^{-1} \text{ cm}^{-2}$). Assuming the validity of Equation 24, K can be related to electrode-kinetic parameters by the

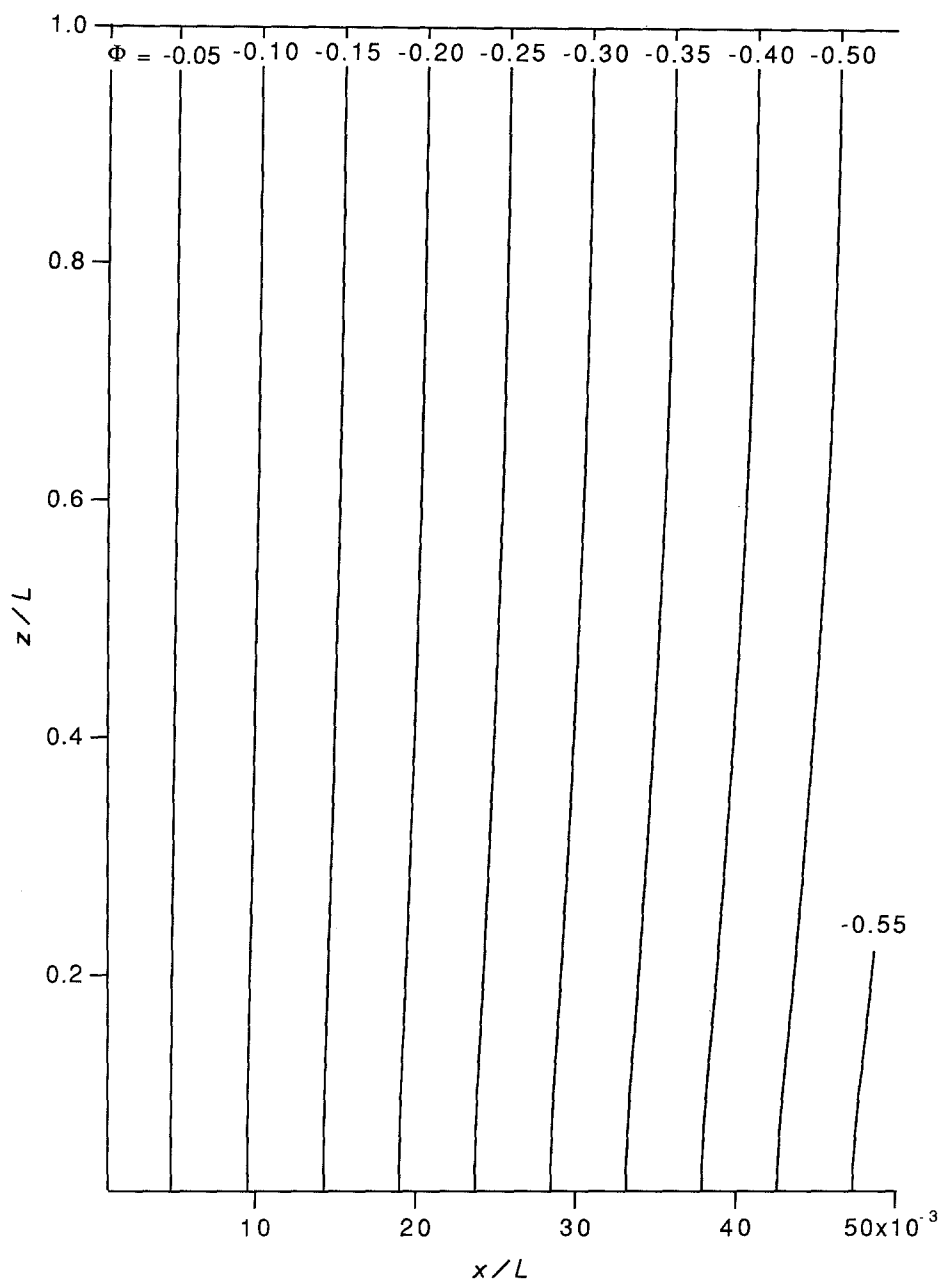


Fig. 3. Equipotentials of the potential distribution calculated from Equation 22, for $x_1/L = 0.05$, $x_2/L = 0.051$, $h/L = 0.01$, $w/L = 0.1$, and $\kappa_2/\kappa_1 = 0.00001$.

equation

$$K = \frac{i_0(\alpha_a + \alpha_c)F}{RT} \quad (27)$$

That Equation 3 is recovered in the limiting case where the reaction resistance tends to zero can be demonstrated dividing by both sides of Equation 26 by K and allowing K to tend to infinity. This formulation of the linearized secondary current distribution problem bears some similarities to a treatment by Scott *et al.* [19] of diffusion through a resistive interface.

3.2. Analytical solution

The steps involved in the solution are closely similar to those described above for the primary current distribution, and the resulting expression is identical in form to Equation 22 except that in this case, the linear

component is

$$\begin{aligned} \Phi_0 &= -\frac{x}{w} & 0 < x < x_1 \\ &= -\frac{x_1}{w} - \frac{LWa}{w} - \frac{\kappa_2}{\kappa_1} \left(\frac{x - x_1}{w} \right) & x_1 < x < x_2 \end{aligned} \quad (28)$$

where Wa is the Wagner number [20] (the ratio of polarization resistance to electrolyte resistance) defined by

$$Wa = \frac{\kappa_2}{LK} \quad (29)$$

and the constants A_m , B_m and C_m are given by the equations

$$A_m = \left[(\sinh(a_m x_1) + m\pi Wa \cosh(a_m x_1)) \right]$$

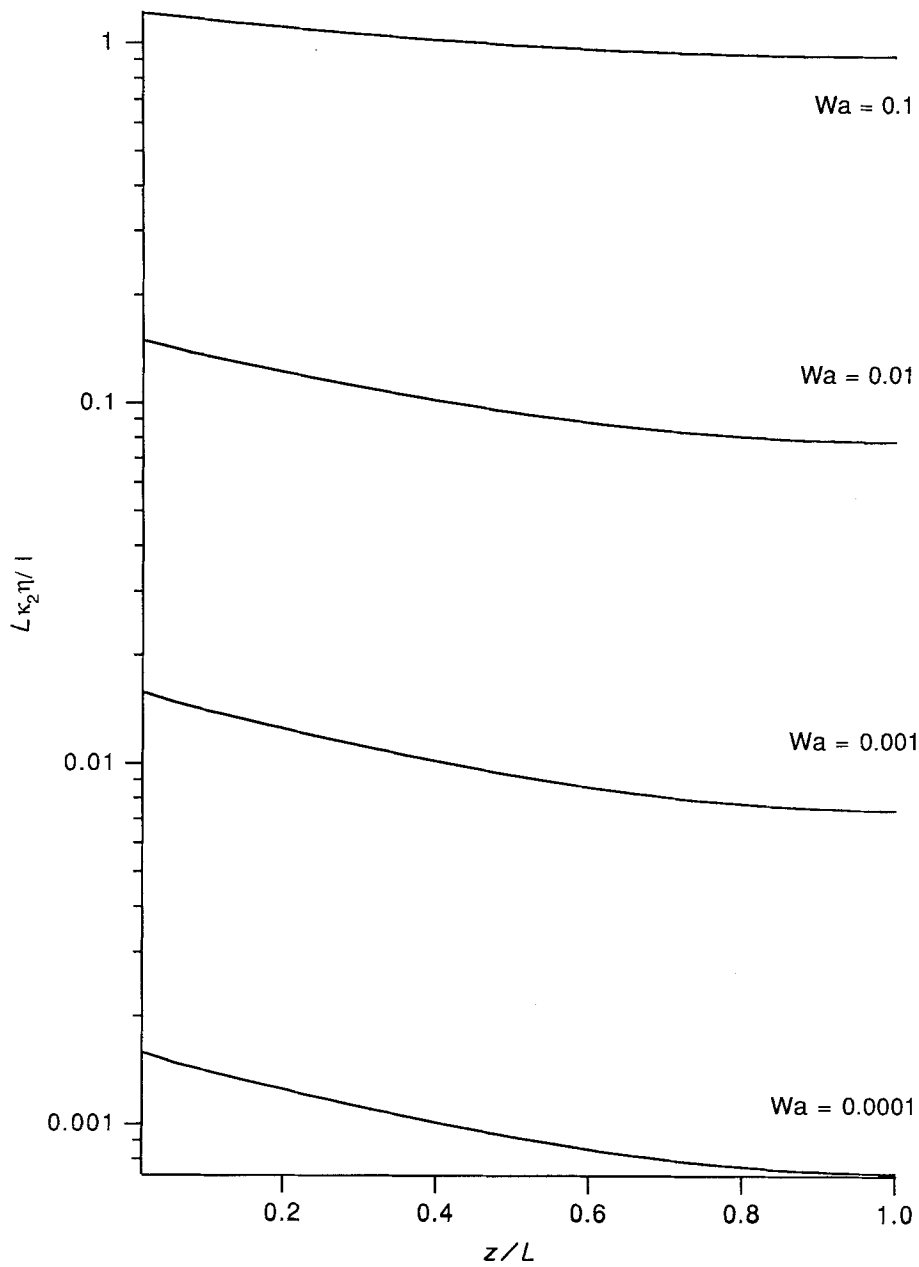


Fig. 4. Profile of overpotential along the electrode-electrolyte interface, for $\kappa_2/\kappa_1 = 0.0001$ and different values of $Wa = \kappa_2/LK$. Geometrical parameters are those used in Fig. 2.

$$\begin{aligned} & \times \cosh(a_m x_1) - \frac{\kappa_2}{\kappa_1} \cosh(a_m x_1) \\ & \times \sinh(a_m x_1) \Big] / a_m D_m \end{aligned} \quad (30a)$$

$$\begin{aligned} B_m = & \left[(\sinh(a_m x_1) + m\pi Wa \cosh(a_m x_1)) \right. \\ & \left. \times \sinh(a_m x_1) - \frac{\kappa_2}{\kappa_1} \cosh^2(a_m x_1) \right] / a_m D_m \end{aligned} \quad (30b)$$

$$C_m = \frac{1}{a_m D_m} \quad (30c)$$

$$\begin{aligned} D_m = & [\sinh(a_m x_1) + m\pi Wa \cosh(a_m x_1)] \\ & \times [\cosh(a_m x_1) \sinh(a_m x_2) - \sinh(a_m x_1) \end{aligned}$$

$$\begin{aligned} & \times \cosh(a_m x_2)] + \frac{\kappa_2}{\kappa_1} [\cosh^2(a_m x_1) \\ & \times \cosh(a_m x_2) - \sinh(a_m x_1) \cosh(a_m x_1) \\ & \times \sinh(a_m x_2)] \end{aligned} \quad (31)$$

For a given set of values of x_1, x_2, w, L and h , the form of the linearized secondary current distribution of the cell may thus be regarded as being determined by the two numbers κ_2/κ_1 and Wa .

A representative value of Wa may be determined by assuming that the sum of the anodic and cathodic transfer coefficients is unity, $i_0 = 0.05 \text{ A cm}^{-2}$, $\kappa_2 = 0.1 \text{ } \Omega^{-1} \text{ cm}^{-1}$, $L = 30 \text{ cm}$ (12 in.) and $T = 27^\circ \text{ C} = 300 \text{ K}$. The slope of the polarization curve is found to be

$$K = \frac{i_0 F}{RT} = 1.93 \text{ } \Omega^{-1} \text{ cm}^{-2} \quad (32)$$

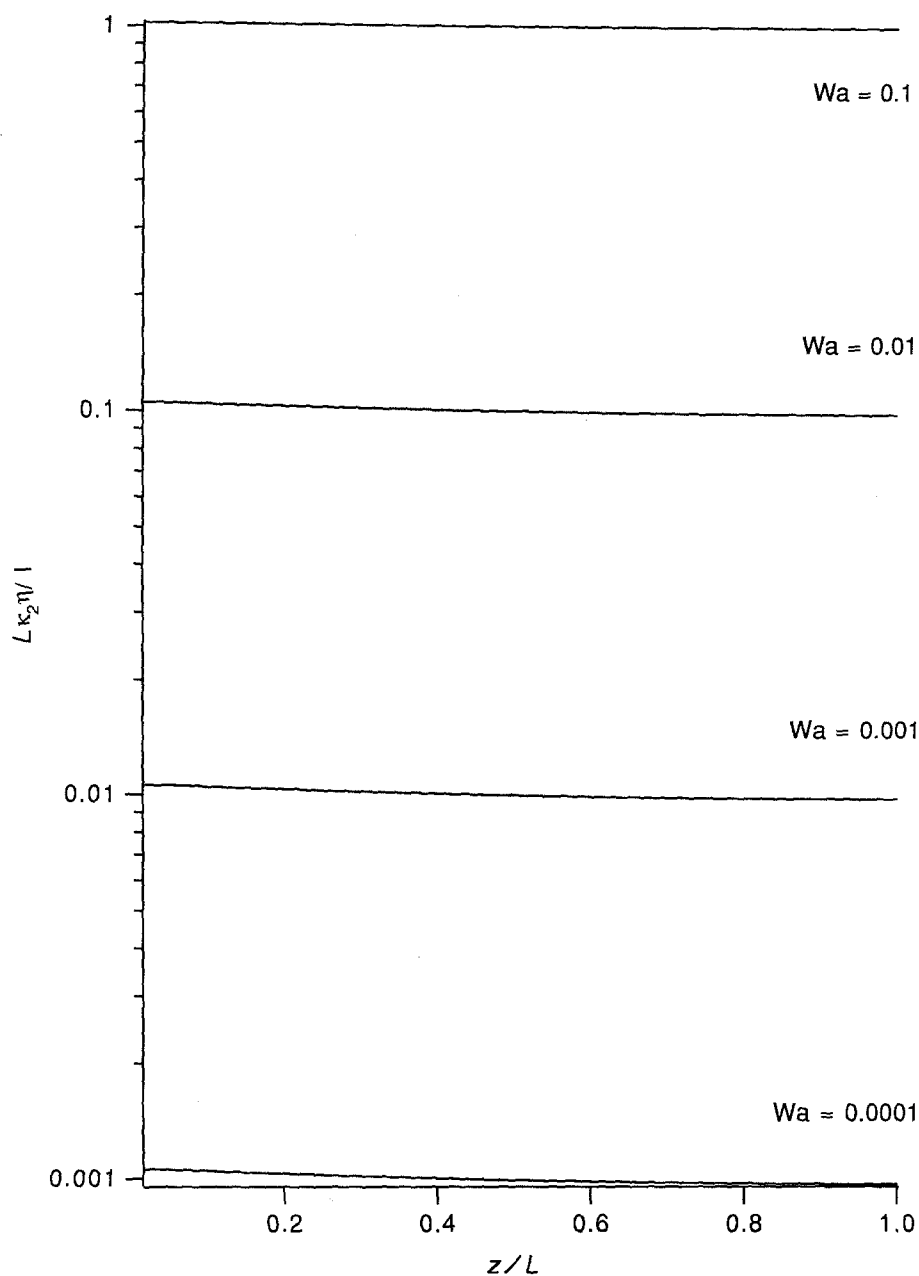


Fig. 5. Profile of overpotential along the electrode-electrolyte interface, for $\kappa_2/\kappa_1 = 0.00001$ and different values of $Wa = \kappa_2/LK$. Geometrical parameters are those used in Fig. 2.

so that

$$Wa = \frac{\kappa_2}{KL} = 1.73 \times 10^{-3} \quad (33)$$

3.4. Calculations

The profile of overpotential along the interface between the electrode and solution is shown in Figs 4 and 5, for conductivity ratios of 0.0001 and 0.00001, respectively. In Fig. 4, the variation of overpotential along the electrode is seen to be quite pronounced, while in Fig. 5, the overpotential variation is very slight. Figures 4 and 5 thus serve to illustrate the combined effect of electrode resistance and reaction resistance on the overpotential profile and hence on the uniformity of reaction along the electrode. Since the form of the overpotential profile is the same for each value of Wa , these results also demonstrate that the most important

parameter influencing the uniformity of overpotential and interfacial current density is the conductivity ratio.

3.5 Comparison with one-dimensional models

In addition to their analytical calculation of the stream function for the two-dimensional current distribution, Tobias and Wijnsman [1] presented a simplified analysis in which current enters the resistive electrode at one end point and one-dimensional current flow is assumed to occur in the electrolyte as well as within the resistive electrode (this and related assumptions form the basis of most subsequently published work on resistive electrode effects, as exemplified by [4]). With this approximation, the current density profile is easily shown to satisfy a Helmholtz-type ordinary differential equation, which in the geometry considered here can readily be solved in

terms of hyperbolic functions. This is essentially different from the approach followed in the present paper, where band contacts of finite width are assumed, but one would expect that for sufficiently small values of h compared with L , the band contacts assumed in the present model would become essentially equivalent to the point contacts assumed in Tobias and Wijsman's work.

We have recently shown that this limiting case is approached closely for $h/L < 0.05$. The details are described in a recently submitted paper [21], which also presents calculations for rectangular cells with two resistive electrodes and an investigation of the effect of relative contact positions on the form of the current distribution within the electrolyte.

4. Conclusions

In this paper, it has been shown how electrode resistance effects in rectangular electrochemical cells can be calculated by solution of Laplace's equation for both the electrolyte and electrode. This procedure does not require the usual assumptions that the resistive electrode is of negligible thickness and that the current distribution within it is one-dimensional. The results can be used to determine the influence of finite electrode thickness and conductivity on the distribution of the current density along the electrode-solution interface. The Fourier series that result from the analysis can readily be applied to calculate the effects of external electrical contact geometry on the current distribution within the electrolyte. In the general case, a y -dependent term in Laplace's equation would have to be included, so that the potential distributions would satisfy

$$\nabla^2 V \equiv \frac{\partial^2 V}{\partial x^2} + \frac{\partial^2 V}{\partial y^2} + \frac{\partial^2 V}{\partial z^2} = 0 \quad (34)$$

and would accordingly contain double Fourier series (with respect to y and z).

In this paper, electrode kinetic effects were assumed to be either absent or satisfactorily described by a linear polarization law. Future work will examine the generalization of these calculations to include non-linear electrode kinetics in the internal boundary conditions for the secondary current distribution.

References

- [1] C. W. Tobias and R. Wijsman, *J. Electrochem. Soc.* **100** (1953) 459.
- [2] B. E. Conway, E. Gileadi and H. G. Oswin, *Can. J. Chem.* **41** (1963) 2447.
- [3] S. K. Rangarajan, M. J. Dignam and B. E. Conway, *ibid.* **45** (1967) 422.
- [4] K. Scott, *J. Appl. Electrochem.* **13** (1983) 209.
- [5] P. M. Robertson, *Electrochim. Acta* **22** (1977) 411.
- [6] R. Alkire and R. Varjian, *J. Electrochem. Soc.* **121** (1974) 622.
- [7] *Idem, ibid.* **124** (1977) 388.
- [8] O. Lanzi and U. Landau, *ibid.* **137** (1990) 1139.
- [9] L. Vaaler, *J. Appl. Electrochem.* **9** (1979) 21.
- [10] I. Rousar, V. Cezner, J. Nejeppsava, M. M. Jaksic, M. Spasojevic and B. Z. Nikolic, *ibid.* **7** (1977) 427.
- [11] J. Bisang and G. Kreysa, *ibid.* **18** (1988) 422.
- [12] J. Bisang, *ibid.* **19** (1989) 500.
- [13] P. Moon and D. E. Spencer, 'Field Theory for Engineers', Van Nostrand, New York (1961).
- [14] R. V. Churchill, 'Fourier Series and Boundary Value Problems', McGraw-Hill, New York (1963).
- [15] C. Lanczos, 'Discourse on Fourier Series', Oliver and Boyd, Edinburgh (1966).
- [16] F. Scheid, 'Theory and Problems of Numerical Analysis', Schaum's Outline Series, McGraw-Hill, New York (1968).
- [17] S. L. Marshall, *J. Electrochem. Soc.* **138** (1991) 1040.
- [18] A. D. Graves, G. J. Hills and D. Inman, in: *Advances in Electrochemistry and Electrochemical Engineering*, Vol. 4, (edited by P. Delahay), (1966) p. 117.
- [19] E. J. Scott, L. H. Tung and H. G. Drickamer, *J. Chem. Phys.* **19** (1951) 1075.
- [20] C. Wagner, *J. Electrochem. Soc.* **98** (1951) 116.
- [21] S. L. Marshall and S. K. Wolff, paper presented at the 8th Australasian Electrochemistry Conference, Auckland, New Zealand, Feb. 1992; *J. Electroanal. Chem.* in press.